

UNCLASSIFIED

CONFIDENTIAL

Copy 6
RM L56G27

C.2



NACA

RESEARCH MEMORANDUM

EXPERIMENTAL AND THEORETICAL STUDIES OF INTERFERENCE

EFFECTS ON THE DAMPING IN ROLL OF THE BELL X-1A

RESEARCH AIRPLANE AT SUPERSONIC SPEEDS

(INCLUDING CANOPY SHAPE EFFECTS)

By Russell W. McDearmon and William B. Boatright

Langley Aeronautical Laboratory
Langley Field, Va.
UNCLASSIFIED

LIBRARY COPY

To _____

OCT 19 1956

By authority of *NASA* *Eff* Date *12-1-57*

LANGLEY AERONAUTICAL LABORATORY
LIBRARY NACA
LANGLEY FIELD, VIRGINIA

CLASSIFIED DOCUMENT

7B 1-28-60
This material contains information affecting the National Defense of the United States within the meaning of the espionage laws, Title 18, U.S.C., Secs. 793 and 794, the transmission or revelation of which in any manner to an unauthorized person is prohibited by law.

NATIONAL ADVISORY COMMITTEE FOR AERONAUTICS

WASHINGTON

October 15, 1956

CONFIDENTIAL

UNCLASSIFIED

~~CONFIDENTIAL~~

NATIONAL ADVISORY COMMITTEE FOR AERONAUTICS

RESEARCH MEMORANDUM

EXPERIMENTAL AND THEORETICAL STUDIES OF INTERFERENCE
EFFECTS ON THE DAMPING IN ROLL OF THE BELL X-1A
RESEARCH AIRPLANE AT SUPERSONIC SPEEDS
(INCLUDING CANOPY SHAPE EFFECTS)

By Russell W. McDearmon and William B. Boatright

SUMMARY

Component interference studies have been made in an attempt to explain the unexpected large loss in damping in roll which occurred in wind-tunnel tests at zero angle of attack for the Bell X-1A research airplane near a Mach number of 2.22 in the investigation of NACA Research Memorandum L55119. The present studies include theoretical calculations of the effect of the body flow field on the wing damping in roll and measurements at test Mach numbers of 1.62, 1.94, 2.22, 2.41, and 2.62 of the contributions of the individual components to the damping in roll. In addition, the effects of various modifications to the dorsal and ventral fins are determined experimentally for the complete airplane configuration.

INTRODUCTION

Recent wind-tunnel studies of the damping in roll of some high-speed aircraft configurations have shown that interference effects can strongly influence the damping of the airplane at some supersonic Mach numbers. Reference 1 shows a serious loss in the damping in roll of the Bell X-1A research airplane near a Mach number of 2.2, and this loss is shown to be predominantly associated with the interference effects of the dorsal and ventral fins. References 2 and 3, which present damping-in-roll measurements for the Douglas D-558-II and Bell X-1E research airplanes, respectively, do not show a similar large loss in damping within the test Mach number range.

In an effort to explain more satisfactorily the results obtained in reference 1, and to gain an insight into the nature of some component interference effects which might influence the damping of an airplane at supersonic speeds, additional experimental and theoretical studies of component interference effects on the damping in roll at zero angle

~~CONFIDENTIAL~~

UNCLASSIFIED

of attack of the X-1A airplane have been conducted. The additional experimental studies, which were conducted in the Langley 9-inch supersonic tunnel, consisted of tests at Mach numbers of 1.62, 1.94, 2.22, 2.41, and 2.62 of the body-wing and body-tail combinations with the dorsal and ventral fins removed, and of the complete configuration with several modifications to the dorsal and ventral fins. The theoretical studies show the effect of the interference flow field of the body on the damping in roll of the wing throughout the Mach number range. In addition, at a Mach number of 2.2, the effect of a modified dorsal fin is investigated theoretically.

SYMBOLS

b	wing span, ft
c	wing chord, ft
C_l	rolling-moment coefficient, $\frac{M_x}{qSb}$
c_l	section rolling-moment coefficient
C_{l_p}	damping-in-roll coefficient, $\frac{\partial C_l}{\partial \frac{pb}{2V}}$, per radian
d	body diameter, ft
M	free-stream Mach number
M_x	rolling moment about the body axis, ft-lb
p	rolling angular velocity, radians/sec
p'	static pressure, lb/sq ft
q	dynamic pressure, $0.7p'_{\infty}M^2$, lb/sq ft
R	Reynolds number based on mean aerodynamic chord of the wing
S	total wing area, including portion submerged in body, sq ft
V	free-stream velocity, ft/sec
V_l	limiting velocity (maximum attainable velocity if flow were expanded into a vacuum), ft/sec

$\left. \begin{array}{l} u \\ v \\ w \end{array} \right\}$ perturbation velocities in the x-, y-, and z-directions,
respectively, ft/sec

x longitudinal coordinate, ft

y spanwise coordinate, ft

z vertical coordinate, ft

α angle of attack, deg

$$\beta = \sqrt{M^2 - 1}$$

ϕ velocity potential

Subscripts:

B due to body

B-l on wing lower surface due to body

B-u on wing upper surface due to body

l lower surface of wing

u upper surface of wing

w across wing surface

w-l on wing lower surface due to wing

w-u on wing upper surface due to wing

y value at spanwise station y

∞ free-stream conditions

Configuration designations:

B body

BW body, wing

BWV body, wing, vertical tail

BWVH body, wing, vertical and horizontal tails
BV body, vertical tail
BVH body, vertical and horizontal tails

APPARATUS AND TESTS

All tests were conducted in the Langley 9-inch supersonic tunnel, which is a continuous-operating, closed-circuit type of wind tunnel in which the temperature, pressure, and humidity can be controlled. The test Mach number is varied by use of interchangeable nozzle blocks which form test sections about 9 inches square.

Figure 1 illustrates the complete 1/62-scale model of the Bell X-1A airplane. Three identical bodies were constructed, one for the BWV and the BWVH configurations, one for the BW configuration, and one for the BV and BVH configurations. The steel wings and the fiberglass plastic tail units were removable so that either could be installed on the desired body. A photograph of the model and the damping-in-roll apparatus installed in the tunnel is shown in figure 2. Reference 1 presents further details concerning the models and balance. The test techniques of this report and reference 1 were basically the same. The modifications to the basic model representing the various complete configurations tested in this report are presented in figure 3.

All models were tested at zero angle of attack and had transition strips of aluminum oxide particles on the various components. The dimensions and locations of the strips are given in figure 1.

The Reynolds number range of the tests varied from about 0.44×10^6 at a Mach number of 1.62 to about 0.24×10^6 at a Mach number of 2.62, based on the mean aerodynamic chord of the wing. However, since all tests were conducted with transition strips on the components, boundary-layer conditions encountered at higher Reynolds numbers were probably simulated. For all tests the humidity of the tunnel air was maintained sufficiently low to insure that condensation effects were negligible.

The accuracy of the experimental data is essentially the same as that given in the precision section of reference 1.

THEORETICAL ANALYSIS

The experimental damping in roll of the Bell X-1A airplane and various combinations of its components was compared with some theoretical predictions in reference 1. These predictions included approximations of the effects of wing-tail interference on C_{lp} . The predictions were rather crude, since body effects were neglected, and the theoretical span load distribution used to determine the vortex model of the wing flow field was for an isolated wing. For the complete configuration and the configuration with body, wing, and vertical tail, the theory of reference 1 failed to predict the severe losses in damping obtained experimentally near a Mach number of 2.22. Rather than attempt to refine the wing-tail interference calculations of reference 1, it was decided to make a theoretical evaluation of the effects of the body flow field on the wing damping in roll in the belief that this would be more informative.

Evaluation of the Body Flow Field by
the Method of Characteristics

Reference 4 explains the method of calculating the flow field about a body of revolution using axisymmetric characteristics. For evaluating the flow field about the X-1A body (with dorsal and ventral fins removed), the tip of the body nose was replaced by a cone of 30° semiapex angle forward of the point where it became tangent to the actual nose contour of the X-1A body. This was done in order that the nose shock would remain attached throughout a representative Mach number range corresponding to the experimental tests. Since the cone angle was arbitrarily chosen to be 30° , the lowest Mach number for which characteristic calculations could be made was 1.71. The calculations were made on electronic automatic computing machines. The lattice-point method of characteristics employed in these calculations determined the properties of the flow at the intersection of each characteristic line. A network of characteristic lines of sufficient density was used to permit the construction of accurate pressure (or Mach number) contours of the body alone throughout the region occupied by the wing. The resulting contours of constant Mach number in the body flow field, and the streamlines indicating the angularity of the flow, are shown in figure 4 superimposed on the plan-form sketch of the body and the wing.

It is interesting to note the accuracy with which the method of characteristics determines the body flow field. For example, compare the location of the calculated body nose shock in figure 4(b) with the location of the nose shock in the appropriate schlieren photograph of figure 5. In both cases the shock barely touches the wing tip. The

schlieren pictures of figure 5 show the main features of the complex flow field of the complete airplane throughout the Mach number range. (See ref. 1 for an explanation of the negligible effect of extraneous shock.)

Calculation of the Wing Damping in Roll When Immersed in the Body Flow Field

After calculating the body flow field, the calculation of the wing damping in roll, when immersed in this body flow field, was accomplished by two techniques. Both techniques depended upon a superposition principle and a more detailed explanation of the methods can be found in appendixes A and B. The first technique simply used the linear theory expression for the pressure coefficient which must be used when combining flow fields that are asymmetrical in v or w . (See, for example, ref. 5.) The expression is:

$$\frac{p' - p'_\infty}{q} = -\frac{2u}{V} - \frac{v^2}{V^2} - \frac{w^2}{V^2} \quad (1)$$

Since the w -term in this equation is 0 for the configuration investigated because of symmetry conditions (see appendix A), the only place the effects of the body flow field appeared in the evaluation of the pressure coefficient was in the v -term. For this particular configuration, the results showed only minute differences from those of the theory for the isolated rolling wing in the free stream and are not presented. However, it is believed that the calculated negligible effect should be pointed out as an aid in assessing the limitations of linear theory when applied to complete airplane configurations.

The second technique that was used for evaluating the effects of the body flow field on the wing damping in roll employed a strip analysis. The rate of change of section rolling-moment coefficient with wing-tip helix angle was calculated for elemental chordwise strips of the wing. (See appendix B.) The values of β_y , V_y , and q_y used in these calculations were obtained from the characteristic calculations of the body flow field. Some resulting variations of section rolling-moment coefficient with span are presented in figure 6. Also shown in figure 6 are some strip-theory variations for the wing alone, for which free-stream values were used for β , V , and q . Mechanical integration of these variations of $\frac{\partial c_l}{\partial \frac{pb}{2V}}$ with $\frac{y}{b/2}$ over both wing panels gave C_{lp} .

Figure 7 shows the theoretical variations in C_{lp} throughout the Mach number range. The linear-theory curve (labeled A) was calculated

by using the method presented in reference 6 and represents the damping of an isolated finite wing in the free stream. This method accounts for wing-tip effect. Curve B represents the variation in C_{lp} for the isolated wing rotating in the free stream as predicted by strip theory. This method does not account for the loss in damping near the wing tip and the difference between curves A and B is due to this inadequacy of strip theory. Curve C is the strip-theory calculation of the damping of the wing in the presence of the body and the shaded portion between curves B and C represents the body effect on the wing damping. Curve C could be shifted by the difference between curves A and B and a better approximation of the damping of the wing in the presence of the body would be obtained. This final step is not indicated in figure 7; however, figure 7 does show that, within the Mach number range of the calculations and above a Mach number of about 1.8, the effect of the body flow field on the wing damping in roll is to slightly increase the damping.

Strip Theory Evaluation of Body—Dorsal-Fin Flow-Field Effects on the Wing Damping

At a Mach number of 2.21 an attempt was made to evaluate the combined effect on the wing damping of a body and a dorsal fin or conduit tunnel with a pointed nose. The method consisted of calculating the flow field of an arbitrary dorsal fin with a pointed nose, superimposing this flow field on the body flow field, and calculating the damping of the wing when immersed in the resultant flow field by the strip theory method of the preceding section. The dorsal-fin flow-field calculations only apply for some arbitrary dorsal fin of unknown but pointed shape, since the flow field assumed was a modification of the body flow field. This modification consisted of appropriately reducing the scale of the body nose and shifting its x- and z-locations to correspond to those of the actual X-1A dorsal fin.

The result of the calculations is denoted by the circular symbol at Mach number 2.21 in figure 7. It can be seen that the effect of this dorsal fin with pointed nose is negligible and that no loss in damping was predicted at a Mach number of 2.21. In the subsequent section it will be shown that no significant loss in damping was obtained experimentally near a Mach number of 2.22 for the complete model with a dorsal fin nose which was more pointed than that of the basic model.

EXPERIMENTAL RESULTS

The experimental phase of the investigations of this report consisted of measurements of C_{lp} at zero angle of attack for the complete model with various modifications to the dorsal and ventral fins, and of measurements of C_{lp} for the body-wing and the body-vertical-tail-horizontal-tail configurations, both with the dorsal and ventral fins removed. Figure 3 defines and tabulates the modifications to the dorsal and ventral fins of the complete model. The test Mach numbers were 1.62, 1.94, 2.22, 2.41, and 2.62. However, the complete model with modifications 5, 6, and 7 was tested only at $M = 2.22$. (The actual testing of the complete model with modification 5 at $M = 2.22$ was carried out in the investigations of reference 1, but is included in this report for completeness.)

The variations of rolling-moment coefficient with wing-tip helix angle obtained in the present investigation are presented in figure 8. In general, the variations were linear. The values of damping in roll were determined by taking the slopes of the curves of C_l against $\frac{pb}{2V}$ for the various configurations.

Figure 9 presents the variations with Mach number of C_{lp} for the complete model and combinations of its components with the dorsal and ventral fins in place. All the data of figure 9 were obtained in the investigation of reference 1. It may be seen in figure 9 that two different values of C_{lp} were obtained at $M = 2.22$ for BWVH. The term "alternate" employed in this figure signifies that a separate dorsal fin was used on the model in the test in which the second value of C_{lp} was obtained. The "alternate" dorsal fin was cast from the same mold as the original dorsal fin; however, small errors in reproduction and installation on the model may have caused its external contour to differ slightly from that of the original. The curve representing the variation of C_{lp} with M for BWVH was faired midway between the two values of C_{lp} at $M = 2.22$.

Figure 9 shows the severe losses in damping in roll which were experienced near $M = 2.22$ by the BWVH and the BWV configurations. It should be noted that neither the minimum values of C_{lp} for the BWVH and the BWV configurations in the vicinity of $M = 2.22$ nor the exact Mach numbers at which they occurred were definitely established. In

view of this uncertainty, the curves were dashed in the Mach number range from 1.94 to 2.41. Figure 9 also shows that no significant reduction in damping was obtained for the BW configuration near $M = 2.22$. Wing-body-tail interference effects on C_{lp} were present to some extent

throughout the Mach number range of the tests and were largest in the Mach number region from 2.22 to 2.41. A notable feature of this interference is the fact that the addition of the horizontal tail to the BWV configuration decreased the damping for Mach numbers less than about 2.3 but increased the damping for Mach numbers greater than about 2.3.

Figure 10 presents the variations with Mach number of C_{lp} for the complete model and combinations of its components with the dorsal and ventral fins removed. Also presented is a variation of C_{lp} with Mach number obtained by adding the contributions to C_{lp} of the BW and BVH configurations. Comparison of this variation with that obtained for the BWVH configuration shows that large effects of wing-body-tail interference on C_{lp} were present for $M > 2.22$, and that these effects were small for $M \leq 2.22$. It should be noted that the large interference effects were opposite in direction to those obtained with the dorsal and ventral fins in place. (See fig. 9.)

A theoretical variation of C_{lp} with Mach number for the body-wing configuration is presented in figure 10. This variation is discussed in a subsequent section of the report.

Comparison of the results presented in figures 9 and 10 shows that the loss in damping experienced by the complete model near $M = 2.22$ is principally due to the dorsal and ventral fins. Furthermore, the dorsal and ventral fins caused a rather large decrease in the damping of the complete model throughout the Mach number range of the tests. The addition of the dorsal and ventral fins had little effect on the damping of the body-wing combination, showing that the losses in damping experienced by the BWVH and the BWV configurations were not caused by the direct effects of the dorsal and ventral fins on the wing. The addition of the dorsal and ventral fins caused decreases in the damping of the body-vertical-tail-horizontal-tail combination at all Mach numbers, but these decreases were of insufficient magnitude to account for the large decreases in damping obtained for the complete model by the addition of the dorsal and ventral fins. Therefore, it must be concluded that the losses in damping experienced by the complete model near $M = 2.22$ resulted from the effects of the dorsal and ventral fins on the body-wing-tail combination, rather than from the direct effects of the dorsal and ventral fins on the individual components.

Figure 11 presents the variations with Mach number of C_{l_p} for the unmodified complete model, the complete model with the dorsal and ventral fins removed, and the complete model with various modifications to the dorsal and ventral fins. The larger differences between the curves in the Mach number region of about 2 to 2.5 are obvious and indicate the sensitivity of the C_{l_p} measurements to component interference effects and changes in the dorsal fin nose shape in this Mach number region. Even small changes in dorsal fin nose shape such as modifications 6 and 7 caused variations in C_{l_p} in this Mach number region.

The data of figure 11 show that, compared with the unmodified configuration, the damping in roll at a Mach number of 2.22 increased regardless of whether the dorsal fin nose was made flatter, rounder, or more pointed. This apparent lack of a consistent trend suggested further checking of the data for the unmodified complete configuration (see alternate-dorsal-fin data of fig. 8), but additional testing only confirmed the fact that the lowest damping resulted with the unmodified configuration.

Comparison of the data for modifications 2 and 3 indicates that for this type of configuration with the midsection of the dorsal fin removed, there was little effect of the dorsal fin nose shape on the damping in roll throughout the Mach number range. Furthermore, it can be seen that this type of configuration sustained a high level of damping throughout most of the Mach number range.

GENERAL DISCUSSION

Some general information of interest to a designer of high-speed aircraft that has been obtained from both the theoretical and experimental phases of the investigations of this report is discussed and summarized in this section.

Since the region of the flow field just behind the body-nose shock contains the largest departure from free-stream conditions, the designer can expect the greatest effect on the damping in roll of a wing in a nonviscous body flow field to occur at flight speeds where this region interacts with a sizable tip region of the wing. According to the theoretical calculations of this report, this interaction increases the damping in roll of the wing. (See fig. 7.) The theory curve of figure 10 is the strip-theory curve of the damping of the wing in the presence of the body, shifted by the difference between linear theory and strip theory of an isolated rolling wing. It should be compared with the experimental curve for the BW configuration. Although

experiment does not show as high damping as that predicted by theory in the Mach number 2.2 region, it is in this region of greatest discrepancy between theory and experiment that the experimental data for the complete configuration show the greatest sensitivity to various dorsal- and ventral-fin modifications. The lack of agreement between theory and experiment is due either to viscous effects or to the simplifying assumptions of the theory. In connection with the latter, it should be remembered that a superposition principle was used even in the two-dimensional-flow region of the wing and that complex interactions such as those which occur in the tip region or near the body-wing juncture were neglected entirely.

It is interesting to note that, based strictly on nonviscous considerations, the dorsal fin nose shock for the unmodified configuration would become attached when the free-stream Mach number reached 2.2. (This was determined by using the measured wedge angle of the flat portion of the nose of the dorsal fin and the local Mach number on the body surface at the nose of the dorsal fin.)

Due to the nature of the experimental results, it was not possible to ascribe the large loss in damping in roll near a Mach number of 2.2 to any one isolated effect. On the contrary, the analysis of the experimental results showed that the largest loss in damping near a Mach number of 2.2 only occurred for all the components in combination (i.e., the body, wing, dorsal and ventral fins, and tail). Therefore, based on the present study, a simple generalized statement cannot be made with regard to what type of configuration to avoid in the design of supersonic aircraft. Neither is it possible to make a simple generalized statement concerning the optimum dorsal fin nose design since all modifications to the dorsal fin nose improved the damping.

Since the theory, even with an accurate evaluation of the body flow field, does not explain the loss in damping near a Mach number of 2.2, even for the relatively simple BW configuration (fig. 10), the importance of experimental damping-in-roll studies for the X-1A airplane is obvious. However, damping-in-roll tests of other types of airplane configurations (such as those produced by modifications 2 and 3) and tests of other airplanes (refs. 2 and 3) have not shown an appreciable loss in damping in the Mach number range from 1.62 to 2.62, and linear theory predictions for isolated wings provided satisfactory estimates of the damping of these models. Thus it appears that, despite the peculiar interference effect on C_{l_p} obtained for the X-1A airplane, linear-theory predictions of C_{l_p} for isolated wings are generally adequate for complete configurations in the Mach number range from 1.62 to 2.62.

CONCLUSIONS

Experimental and theoretical studies of component interference effects on the damping in roll of the Bell X-1A research airplane at zero angle of attack and experimental studies of various dorsal-fin and ventral-fin modifications have indicated the following conclusions:

1. The severe loss in damping in roll near a Mach number of 2.2 which is shown in NACA Research Memorandum L55119 to be associated with the presence of the dorsal and ventral fins was found to occur only for all the components in combination. This severe loss was not a direct effect of either the body and the dorsal and ventral fins on the wing or of the body and the dorsal and ventral fins on the tail.
2. Modifying the dorsal fin nose by making it either pointed, rounder, or flatter, resulted in increases in the damping in roll in the Mach number 2.2 region compared with the damping of the unmodified configuration.
3. The greatest increase in the damping of the complete configuration near a Mach number of 2.2 occurred for the dorsal-fin modification which consisted of removing a section of the connecting fin between the vertical tail and the nose such that the resulting configuration resembled an airplane with a bubble canopy in its usual forward location.
4. The theory and the experiment for the body-wing configuration with dorsal and ventral fins removed gave excellent agreement at Mach numbers below about 2.0 and at the maximum Mach number of the tests (2.62); however, at Mach numbers between about 2.0 and 2.5, theory indicates more damping for the body-wing configuration than for the wing alone, whereas experimental results show slight losses in damping. This is the Mach number range wherein the greatest body effect on the wing damping is predicted and coincides with the range where the experimental measurements for the complete configuration show the greatest sensitivity to dorsal fin nose modifications.
5. A theoretical estimate at a Mach number of 2.2 of the combined effect of a body and an arbitrary dorsal fin with a pointed nose on the wing damping in roll showed that the contribution of this dorsal fin to the wing damping was negligible and showed no loss in damping at a Mach number of 2.2. Experimental data also showed only a very slight loss in damping near a Mach number of 2.2 for the complete model with a dorsal fin nose which was more pointed than that of the Bell X-1A airplane.

Langley Aeronautical Laboratory,
National Advisory Committee for Aeronautics,
Langley Field, Va., July 11, 1956.

APPENDIX A

LINEAR-THEORY EVALUATION OF THE BODY FLOW FIELD

EFFECTS ON THE WING DAMPING IN ROLL

As mentioned in the text, the linear-theory expression for the pressure coefficient which must be used when dealing with flow fields that are asymmetrical in v or w is

$$\frac{p' - p'_\infty}{q} = -\frac{2u}{V} - \frac{v^2}{V^2} - \frac{w^2}{V^2} \quad (A1)$$

A discussion of the proper use of this equation is given in reference 5. For a lifting or rolling wing and a body whose cross section increases with x , the perturbation velocities on the upper and lower wing surfaces have the following directions:

$$u_{W-u} = -u_{W-l}$$

$$u_{B-u} = u_{B-l}$$

$$v_{W-u} = -v_{W-l}$$

$$v_{B-u} = v_{B-l}$$

and

$$w_{B-u} = w_{B-l} = 0$$

Therefore, it can be shown that the pressure difference across the wing surface is

$$\frac{p'_l - p'_u}{q_\infty} = -\frac{4u_w}{V} - \frac{4v_B v_w}{V^2} - 0 \quad (A2)$$

This formula was used to evaluate the damping in roll of the body-wing combination. Reference 6 presents in closed form the expressions for the potential ϕ , and the perturbation velocities u_w that apply for the isolated rolling wing for this airplane. The expressions for v_w were determined by differentiating the expressions for ϕ with respect to y . The values of v_B were determined from the results of the

calculations of the body flow field using the method of characteristics. The technique for evaluating the damping of the wing in the body flow field was to evaluate the chordwise lifting-pressure coefficient at various span stations along the wing, to integrate mechanically to determine the span load distribution, and then to integrate the span load distribution curve mechanically to determine C_{lp} .

APPENDIX B

STRIP THEORY EVALUATION OF THE BODY FLOW FIELD

EFFECT ON THE WING DAMPING IN ROLL

The rolling moment on an elemental strip is given by the equation:

$$\frac{dM_x}{q_y} = \frac{\Delta p'}{q_y} y c_y dy = \frac{4\alpha_y}{\beta_y} y c_y dy = \frac{4p}{\beta_y V_y} y^2 c_y dy \quad (B1)$$

where the subscript y denotes the average value of the parameter over a strip which is located at a distance y from the body axis. It follows then that the equation for the rate of change of section rolling-moment coefficient with wing-tip helix angle for a chordwise strip is

$$\frac{\partial c_l}{\partial \frac{pb}{2V}} = \frac{8V_\infty q_y y^2 c_y dy}{S b^2 q_\infty \beta_y V_y} \quad (B2)$$

Evaluation of equation (B2) was accomplished by plotting β_y and V_y along each strip (determined from the body flow field calculations), then integrating mechanically to obtain the average value for each strip. Since the body flow field calculations determined the pressure and the Mach number along each strip, their average values were used to determine q_y/q_∞ . After plotting the spanwise load distribution, the integral was evaluated mechanically to determine C_{lp} . It was not necessary to account for the stream angularity since the correction to β_y , V_y , or M_y appeared only as a cosine function. For the maximum values of stream angularity which occurred in the body flow field (about 4°), this correction was negligible.

REFERENCES

1. McDearmon, Russell W., and Clark, Frank L.: Wind-Tunnel Investigation of the Damping in Roll of the Bell X-1A Research Airplane and Its Components at Supersonic Speeds. NACA RM L55I19, 1956.
2. McDearmon, Russell W.: Wind-Tunnel Investigation of the Damping in Roll of the Douglas D-558-II Research Airplane and Its Components at Supersonic Speeds. NACA RM L56F07, 1956.
3. McDearmon, Russell W., and Clark, Frank L.: Wind-Tunnel Investigation of the Damping in Roll of the Bell X-1E Research Airplane and Its Components at Supersonic Speeds. NACA RM L56B15, 1956.
4. Ferri, Antonio: Application of the Method of Characteristics to Supersonic Rotational Flow. NACA Rep. 841, 1946. (Supersedes NACA TN 1135.)
5. Heaslet, Max A., and Lomax, Harvard: The Calculation of Pressure on Slender Airplanes in Subsonic and Supersonic Flow. NACA Rep. 1185, 1954. (Supersedes NACA TN 2900.)
6. Harmon, Sidney M., and Jeffreys, Isabella: Theoretical Lift and Damping in Roll of Thin Wings With Arbitrary Sweep and Taper at Supersonic Speeds - Supersonic Leading and Trailing Edges. NACA TN 2114, 1950.

Wing:	
Area	4.864 sq in.
Span	5.420 in.
Aspect ratio	6
Section	NACA 65-008 ($\alpha=1$)
Root incidence	2.5°
Tip incidence	1.5°

Horizontal tail:

Area	0.974 sq in.
Section	NACA 65-006

Vertical tail:

Area	0.958 sq in.
Section	NACA 65-008

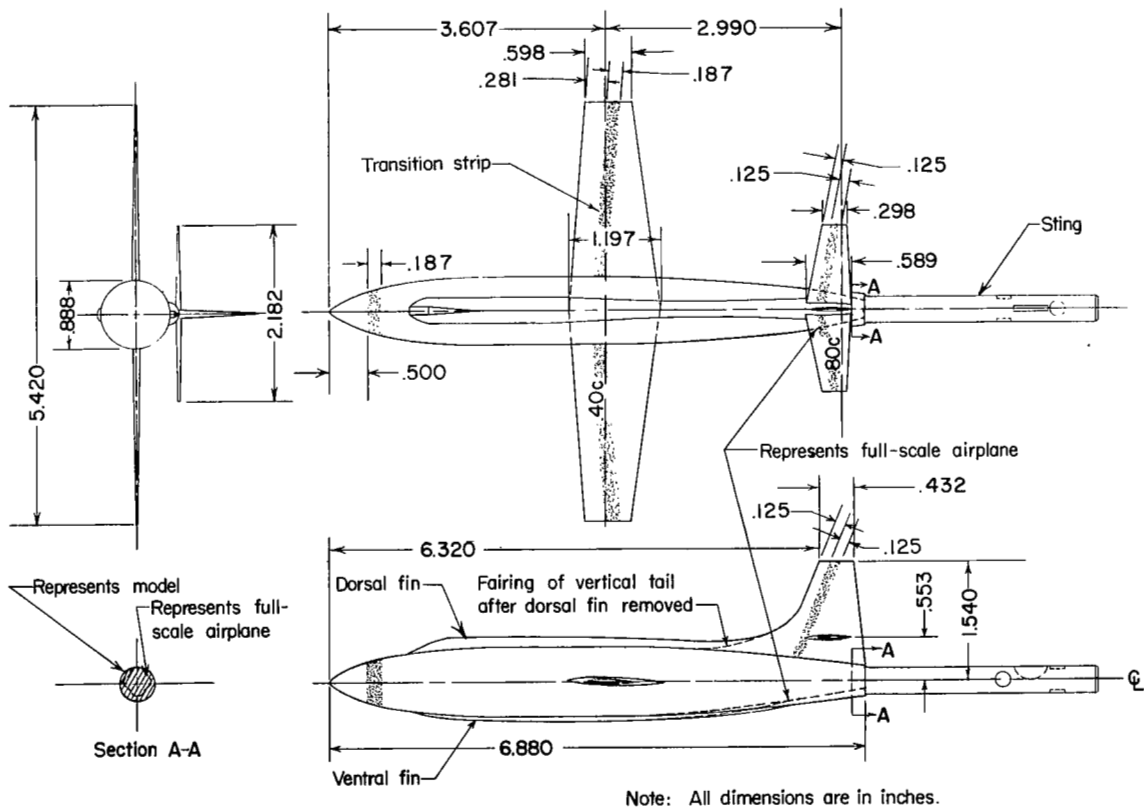
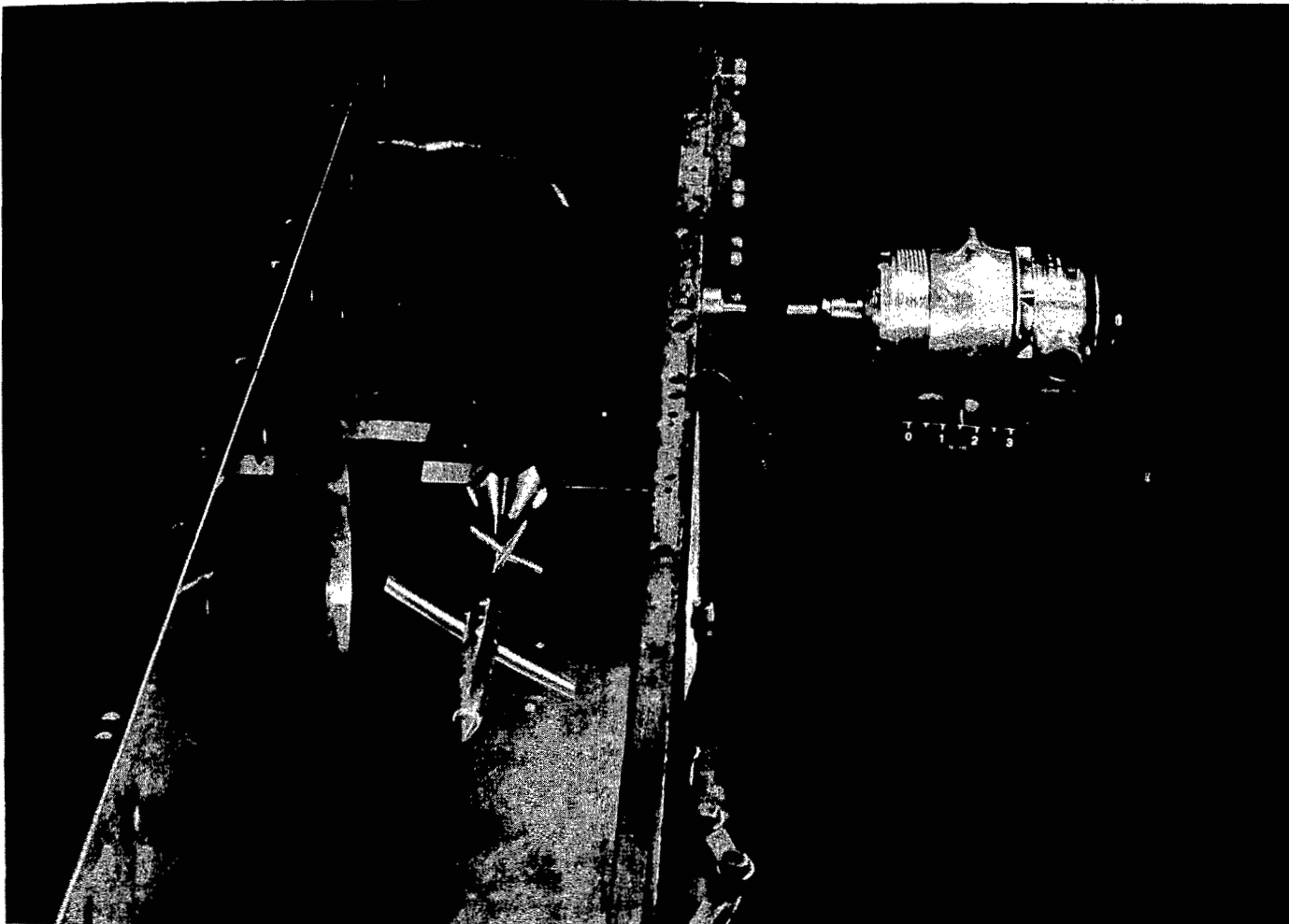


Figure 1.- Drawing of the 1/62-scale basic model.



L-89408
Figure 2.- Photograph of model and damping-in-roll apparatus installed
in tunnel. (Top nozzle block removed.)

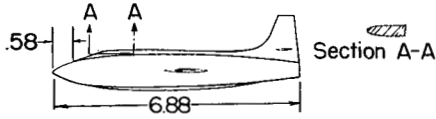
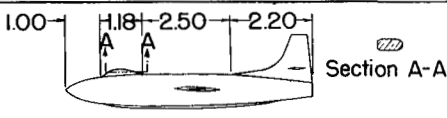
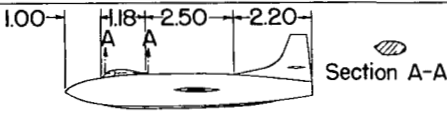



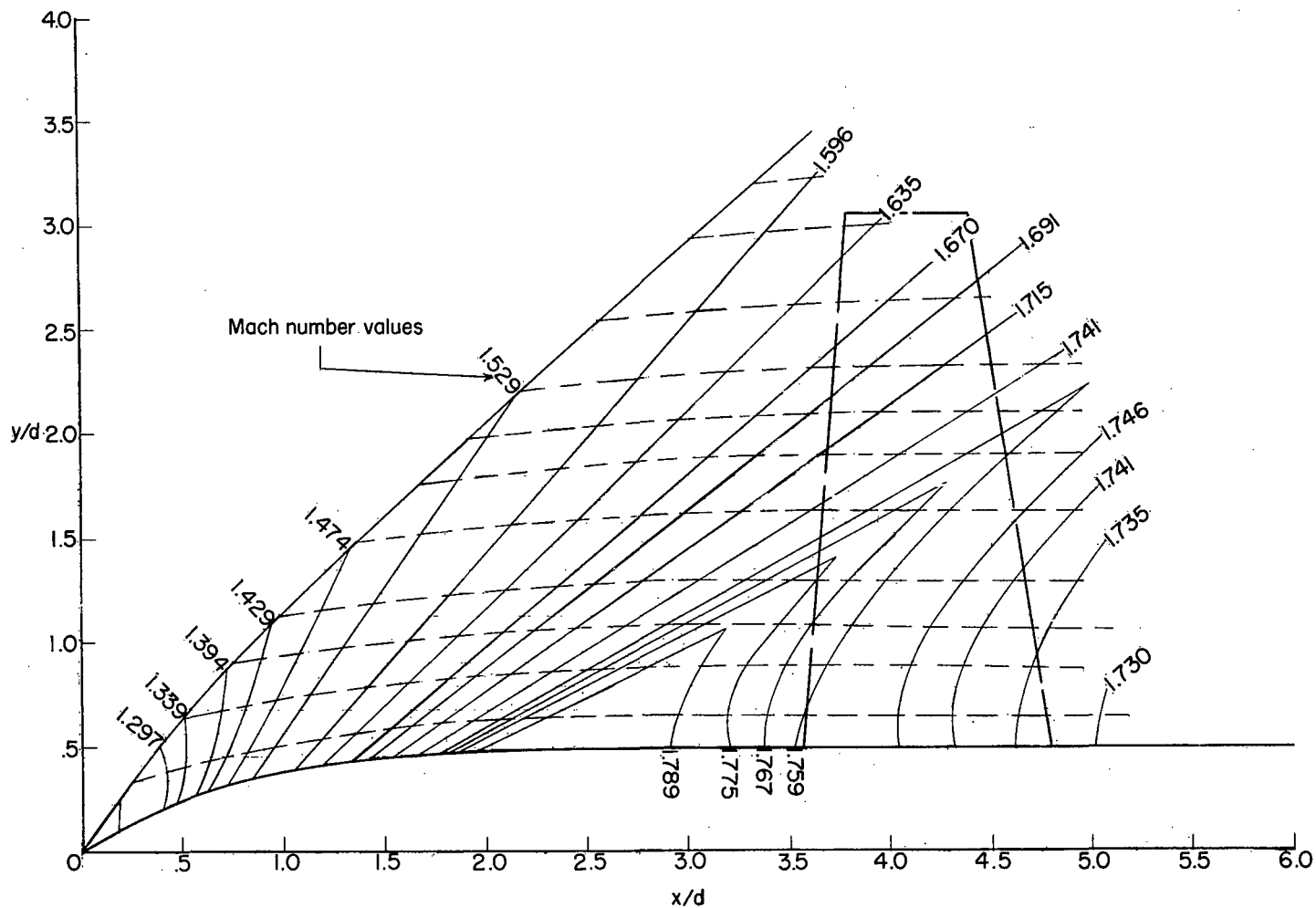
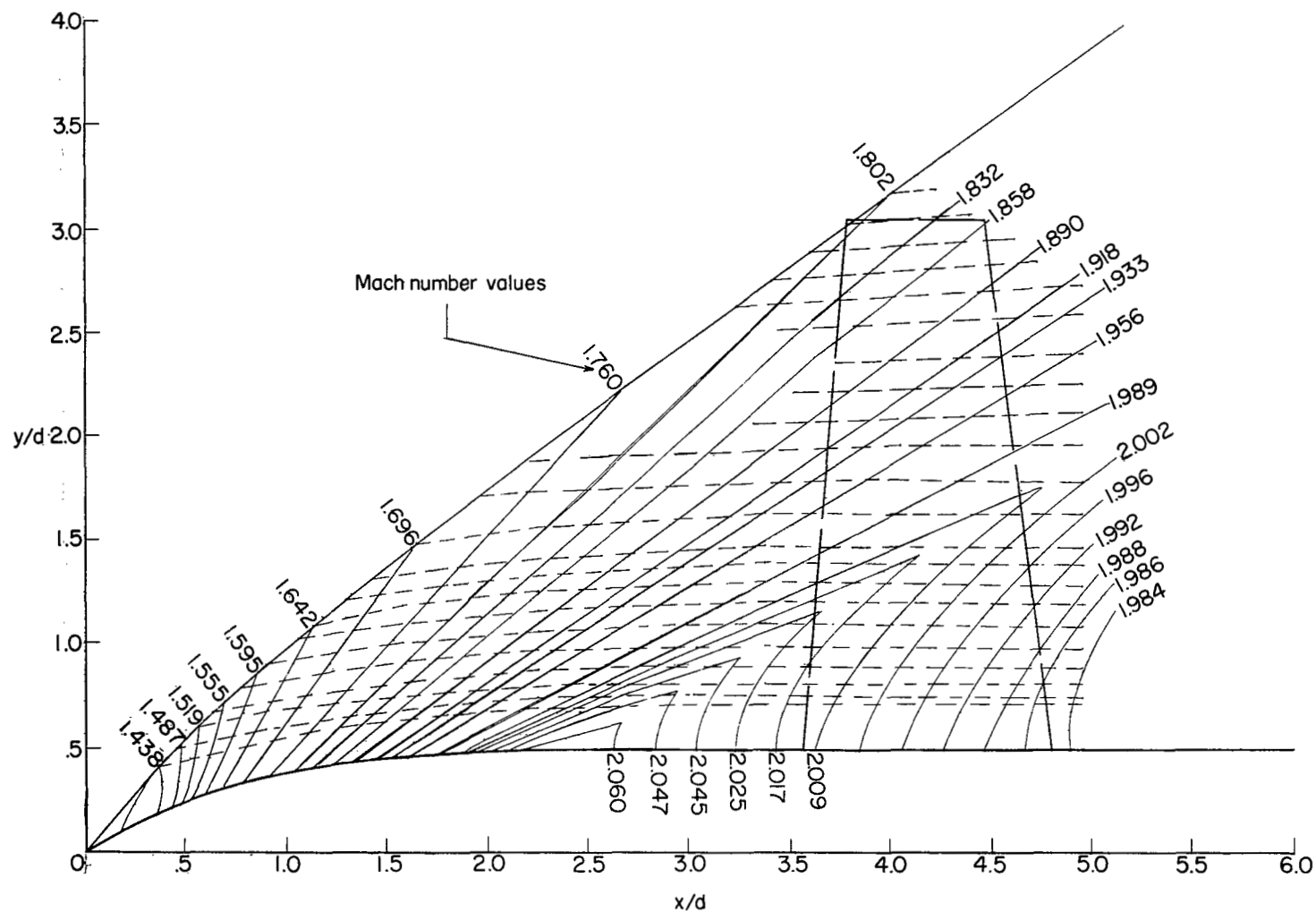
MODIFICATION	SKETCH	DESCRIPTION OF MODIFICATION
1		Nose of dorsal fin was extended and made more pointed than that of the basic model.
2		Original dorsal fin had section removed between nose and vertical tail. Nose shape was the same as in figure 1.
3		Section of dorsal fin removed between nose and tail, and a wedge shaped nose was used.
4		Ventral fin removed; same dorsal fin as in figure 1.
5		Dorsal fin removed.
6		Same as figure 1, except dorsal fin nose was slightly more rounded.
7	<p>Same as modification 6 in sideview.</p>	Same as figure 1, except dorsal fin nose was slightly more flattened.

Figure 3.- Modifications to the basic Bell X-1A model.



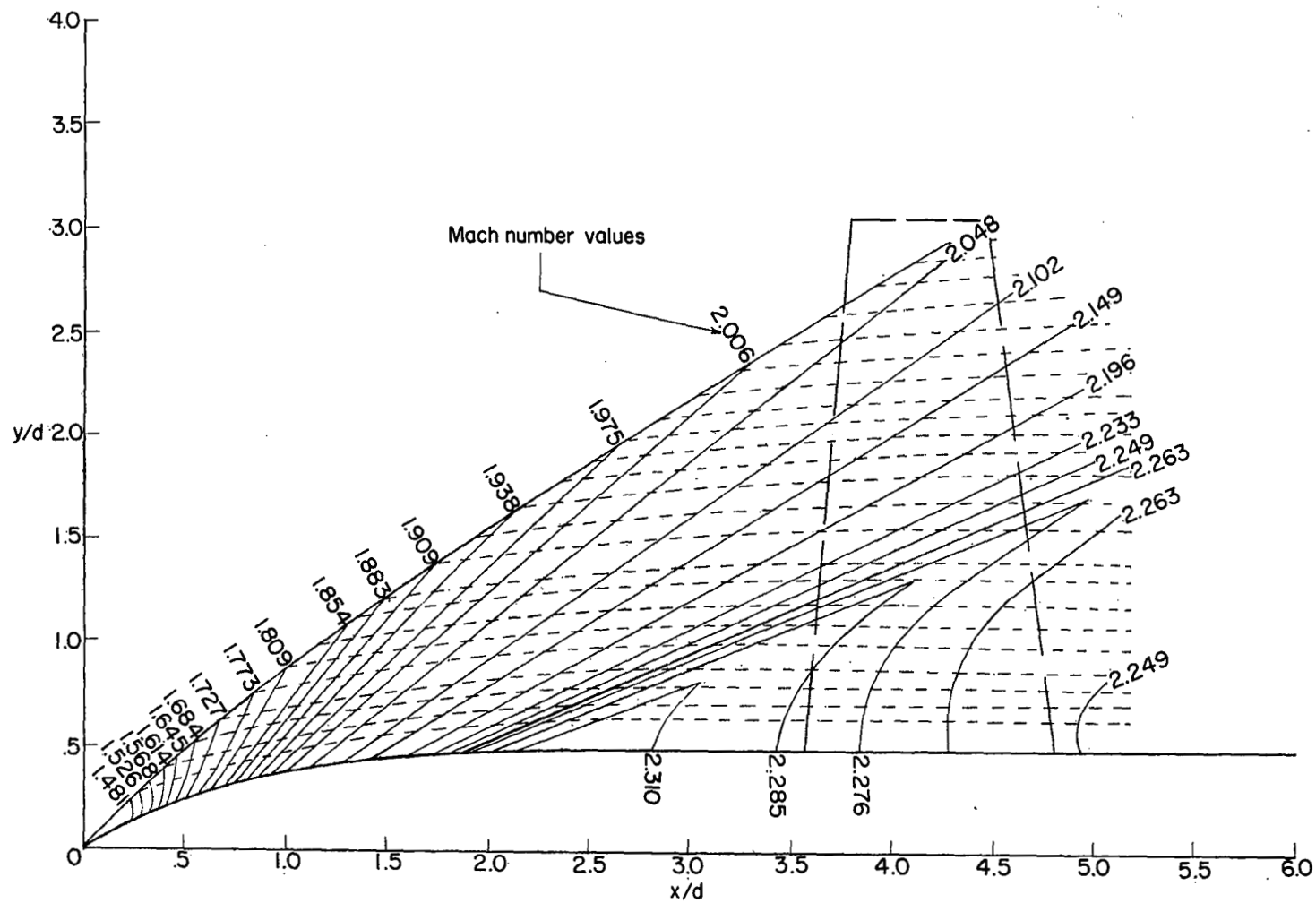
(a) $M = 1.71$.

Figure 4.- Contours of constant Mach number (or pressure) and streamlines in the X-1A body flow field.



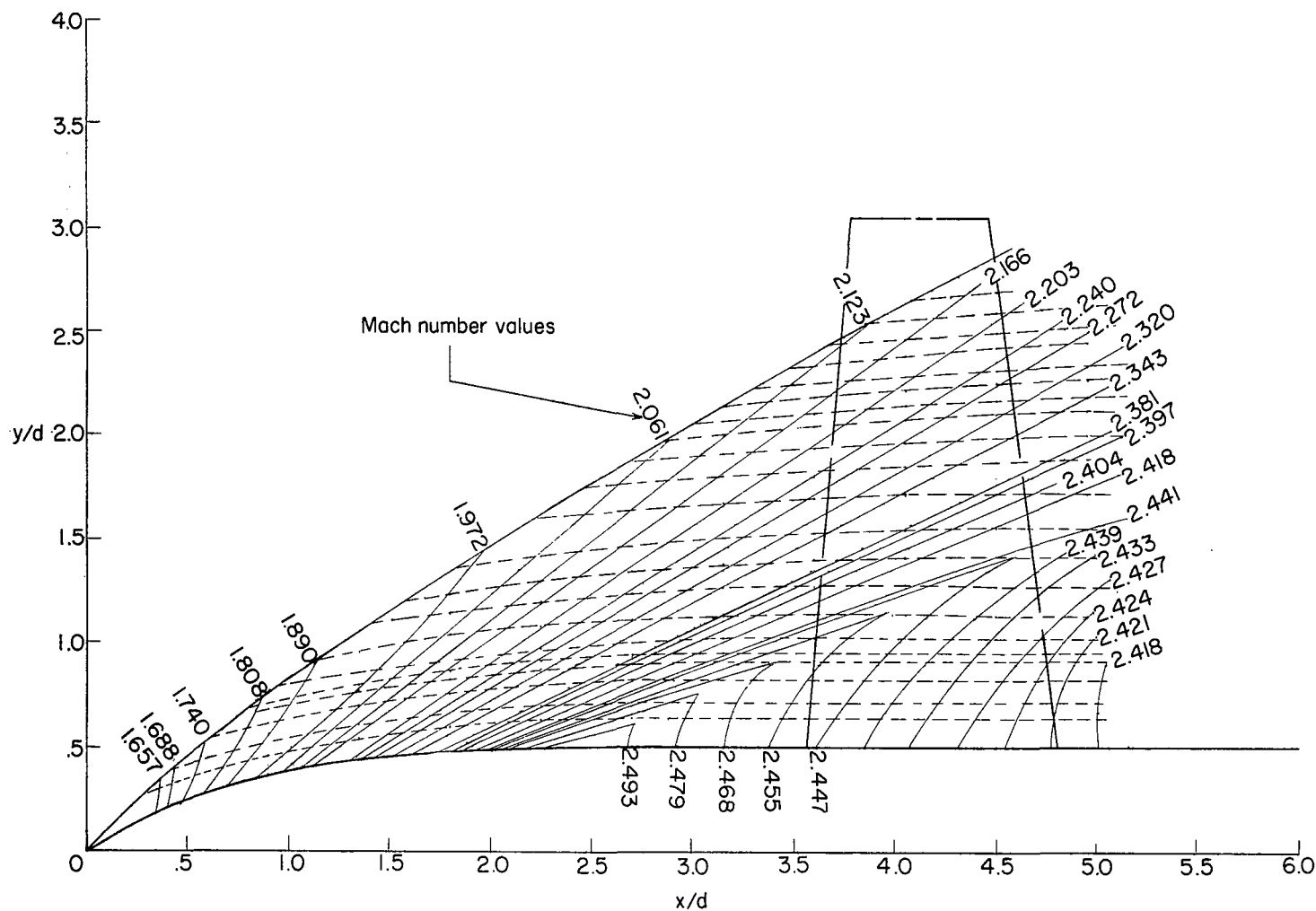
(b) $M = 1.95$.

Figure 4.- Continued.



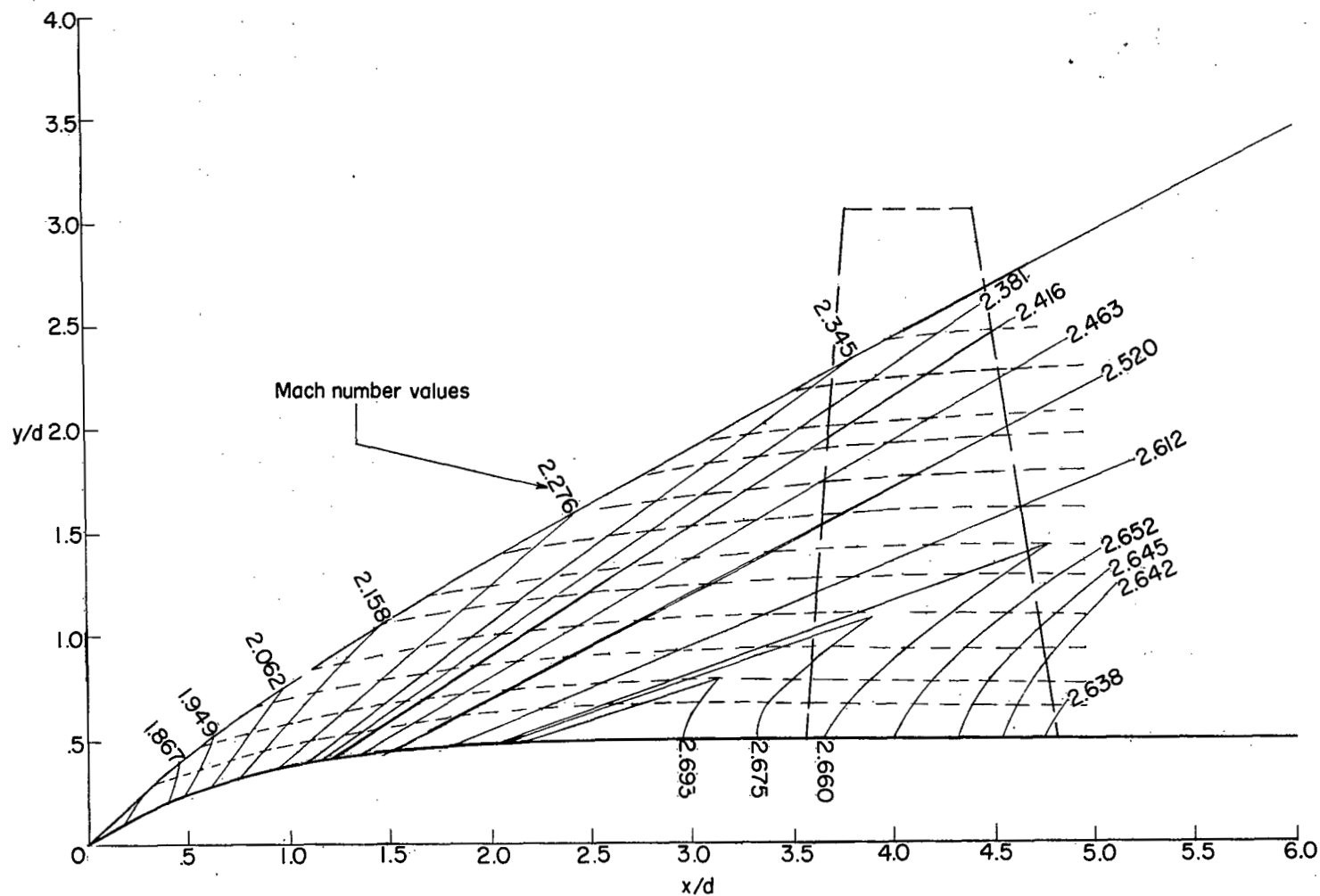
(c) $M = 2.21$.

Figure 4.- Continued.



(d) $M = 2.38$.

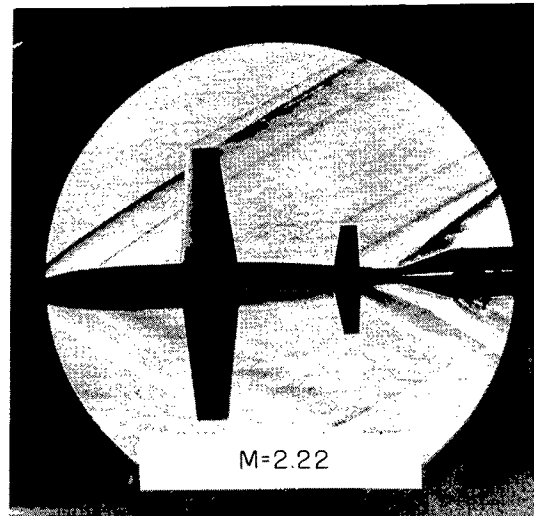
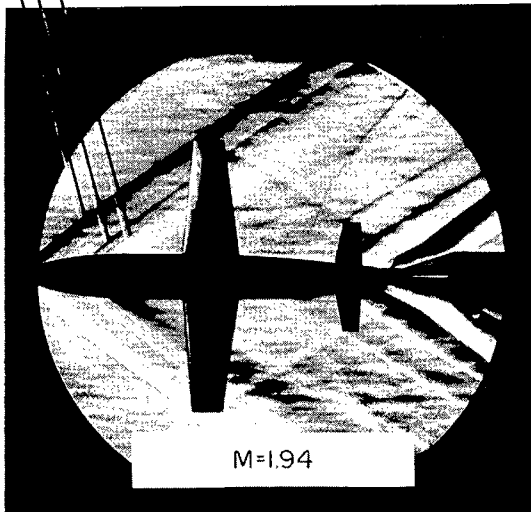
Figure 4.- Continued.



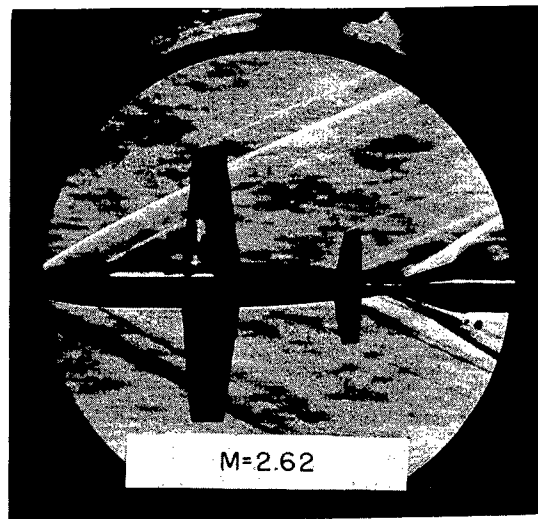
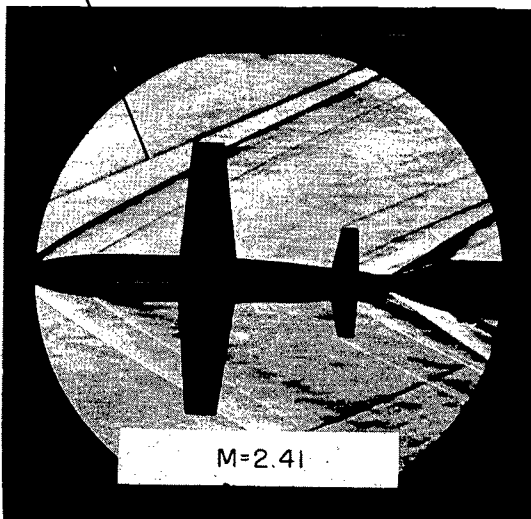
(e) $M = 2.59$.

Figure 4.- Concluded.

Shock wave from body nose
Shock wave from dorsal-fin nose
Shock wave from ventral-fin nose



Extraneous shock wave



L-89391
Figure 5.- Schlieren photographs of the flow about the complete model at zero rolling velocity.

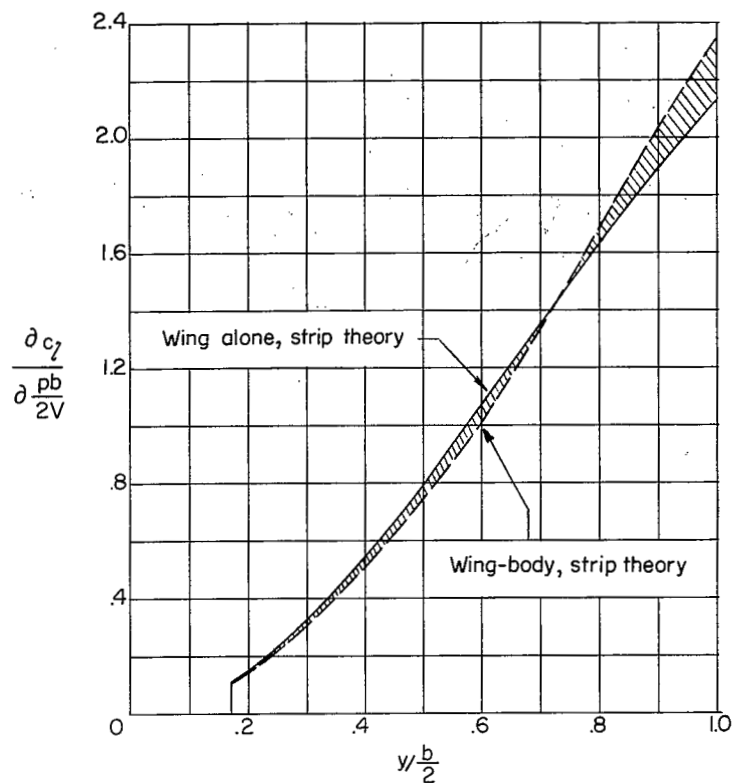
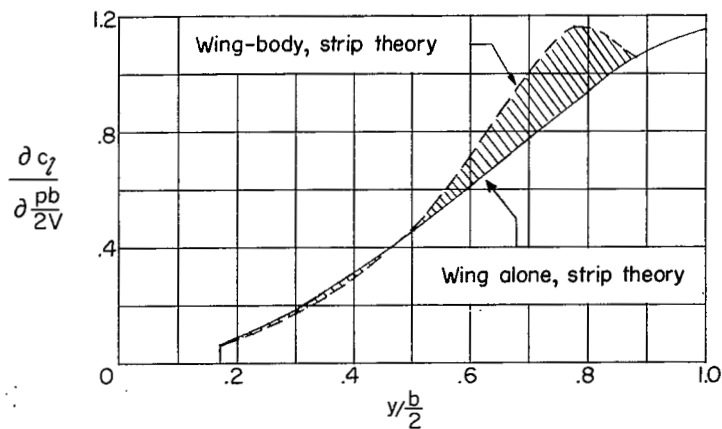
(a) $M = 1.71$.(b) $M = 2.59$.

Figure 6.- Typical theoretical spanwise variations of section rolling-moment coefficient for the rolling X-1A wing showing the body flow field effect.

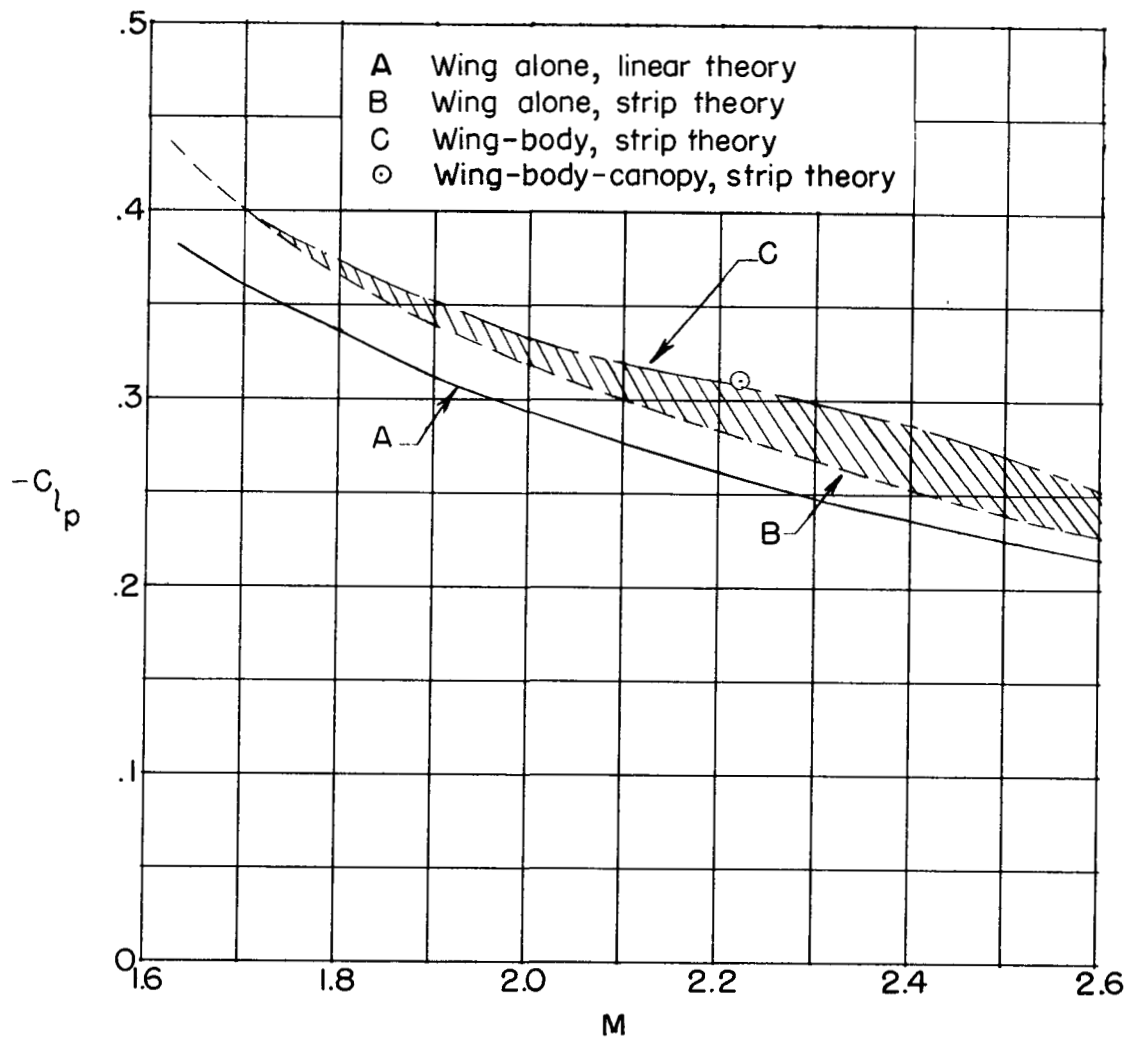


Figure 7.- Comparison of the variations of estimated C_{lp} with Mach number for the various theoretical methods.

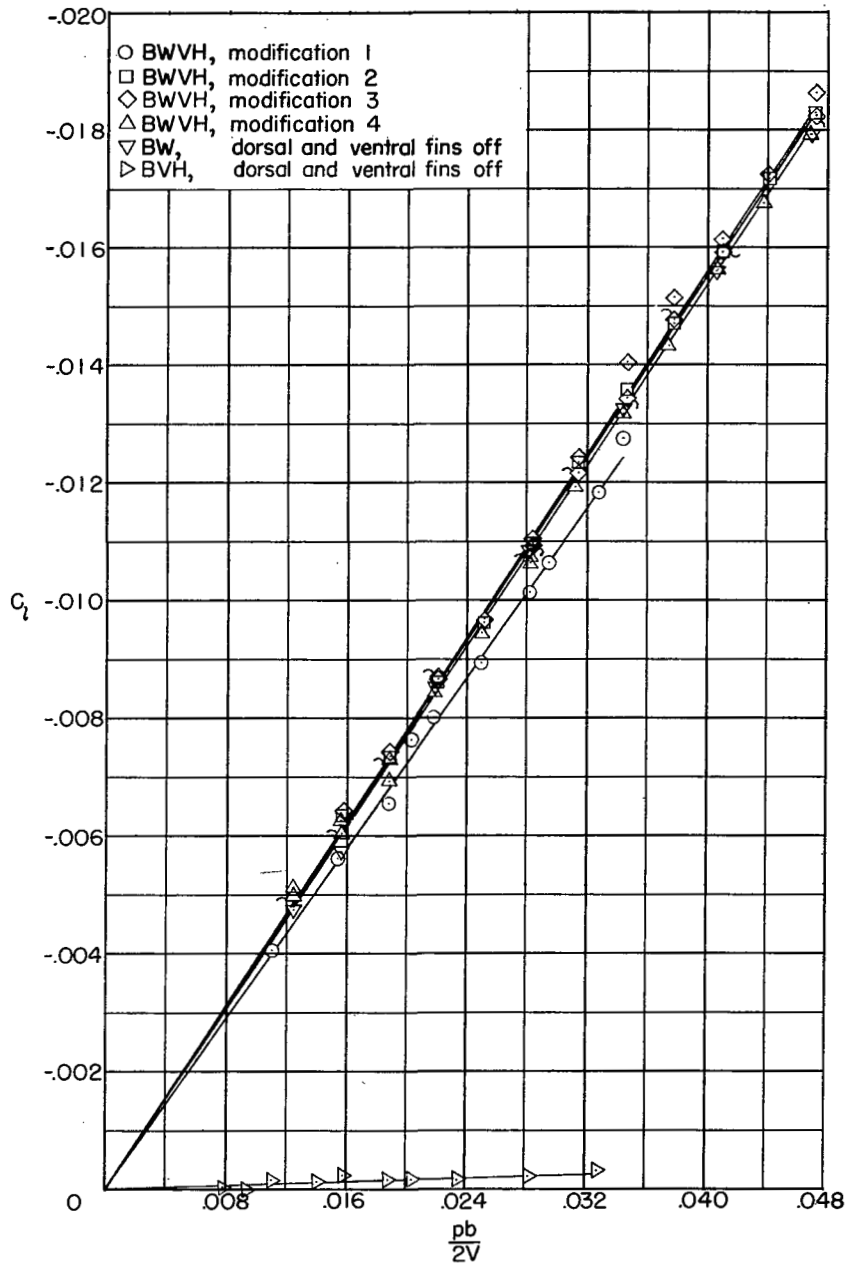
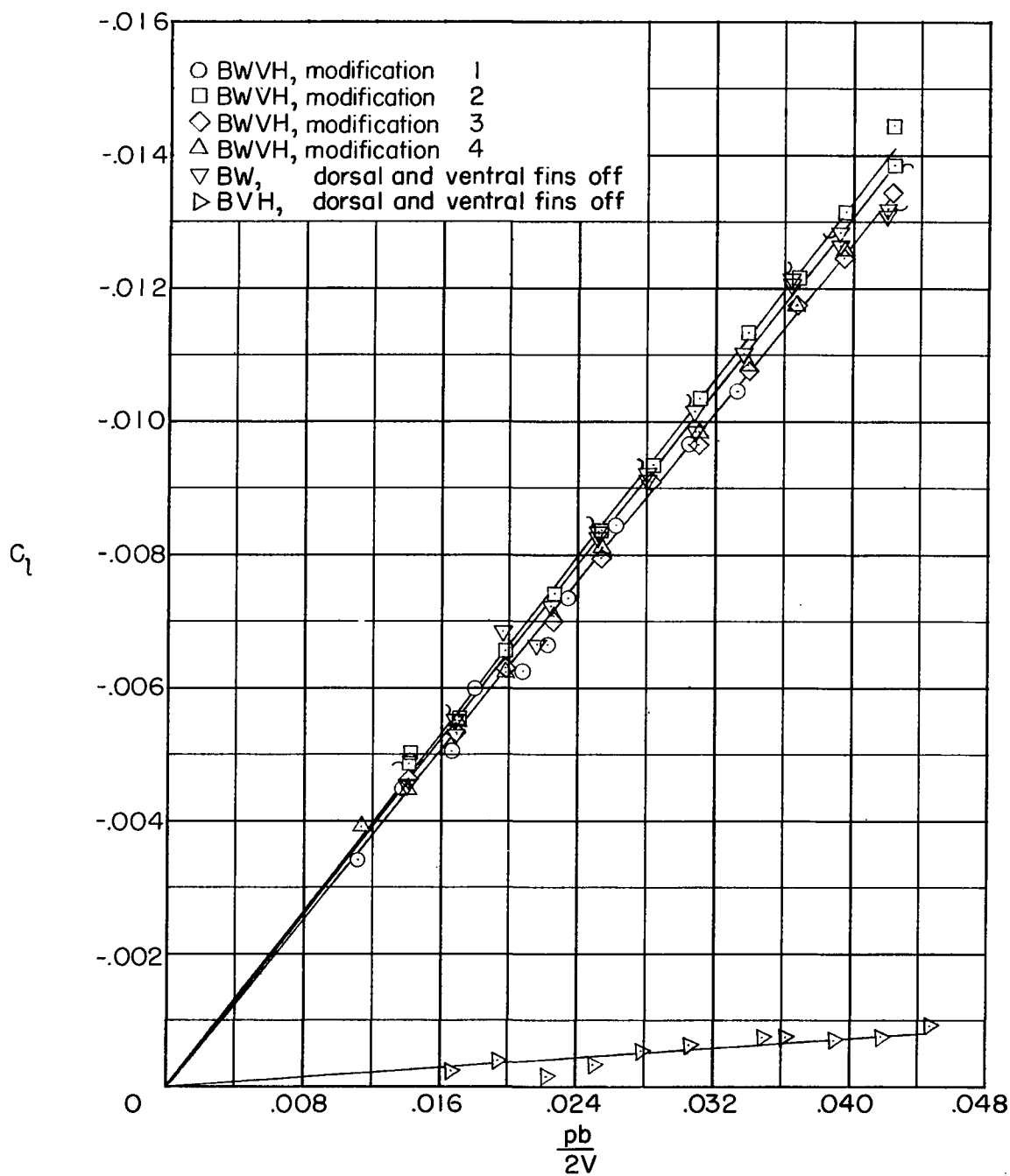
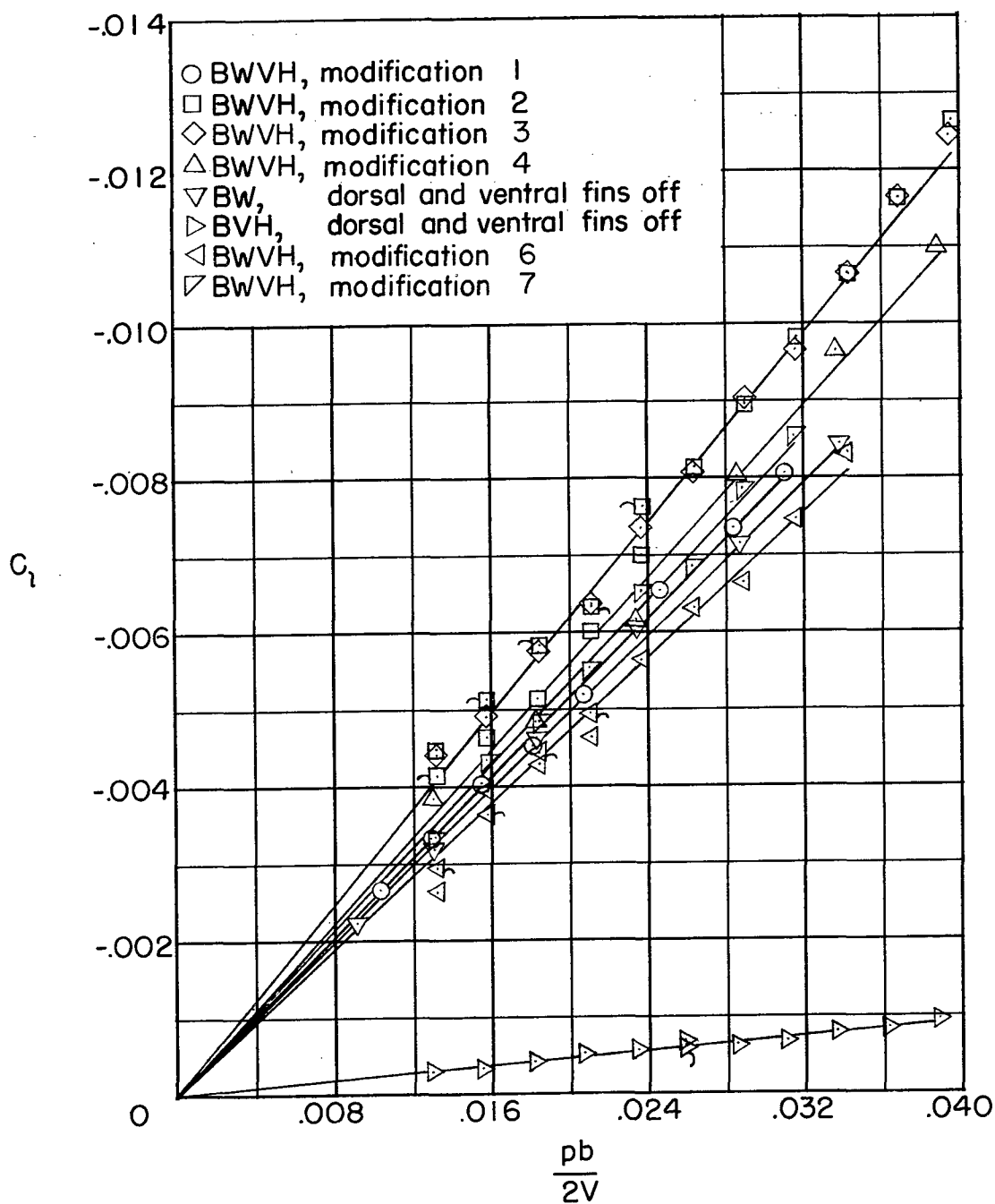
(a) $M = 1.62$.

Figure 8.- Variations of rolling-moment coefficient with wing-tip helix angle for BWVH with various modifications to the dorsal and ventral fins and for BW and BVH with the dorsal and ventral fins removed, at zero angle of attack. Flagged symbols indicate check points.



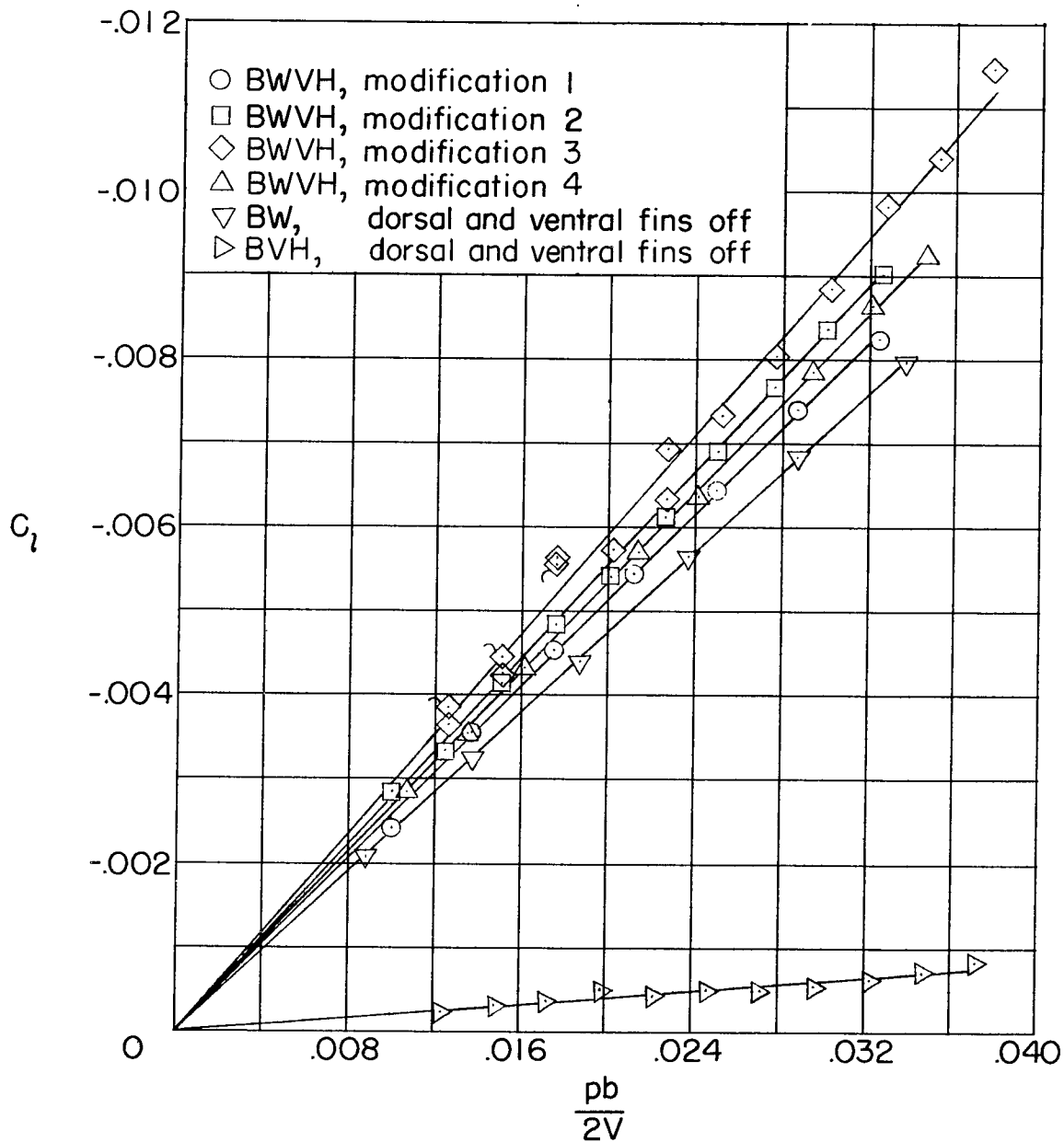
(b) $M = 1.94$.

Figure 8.- Continued.



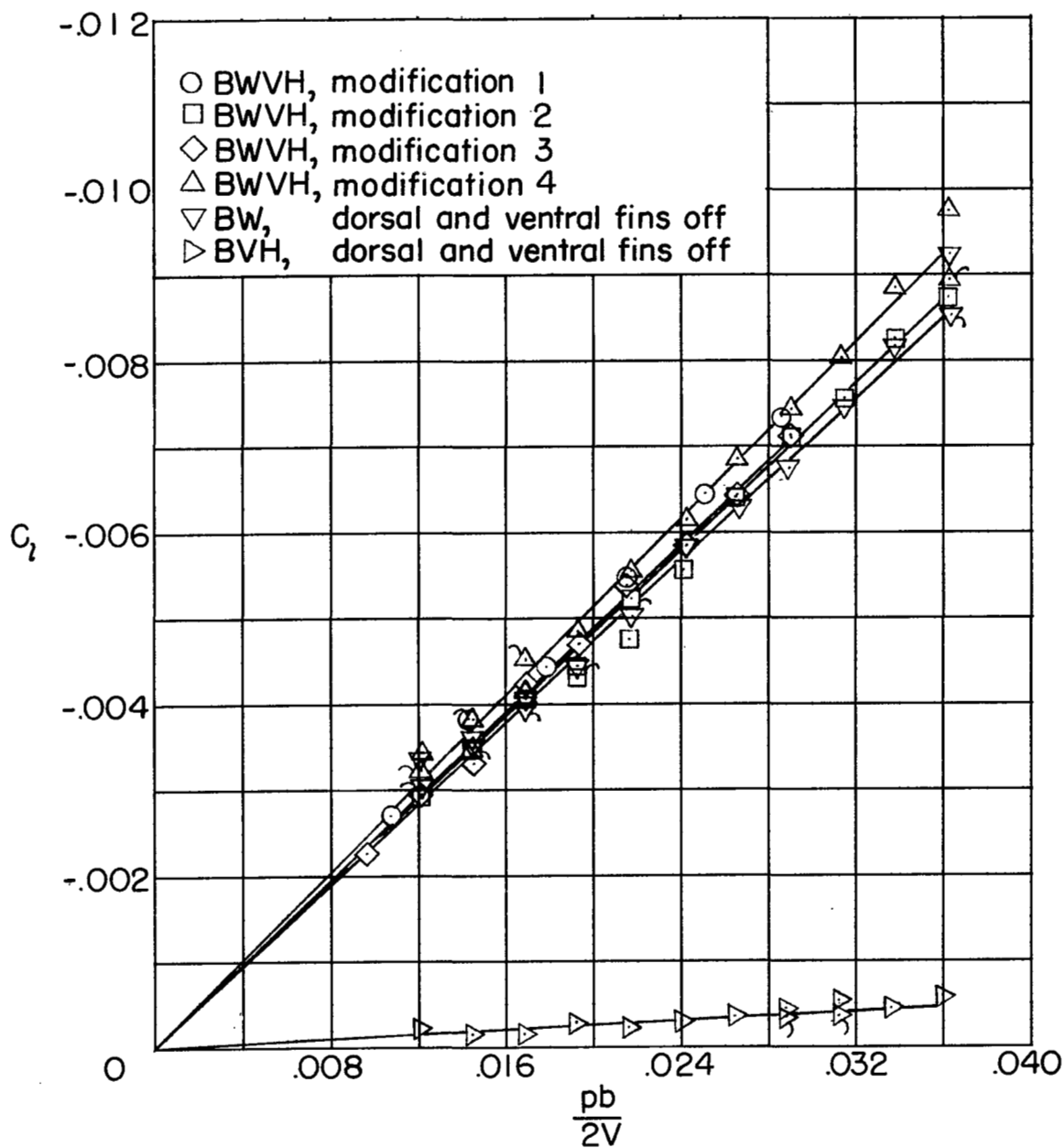
(c) $M = 2.22$.

Figure 8.- Continued.



(d) $M = 2.41$.

Figure 8.- Continued.



(e) $M = 2.62$.

Figure 8.- Concluded.

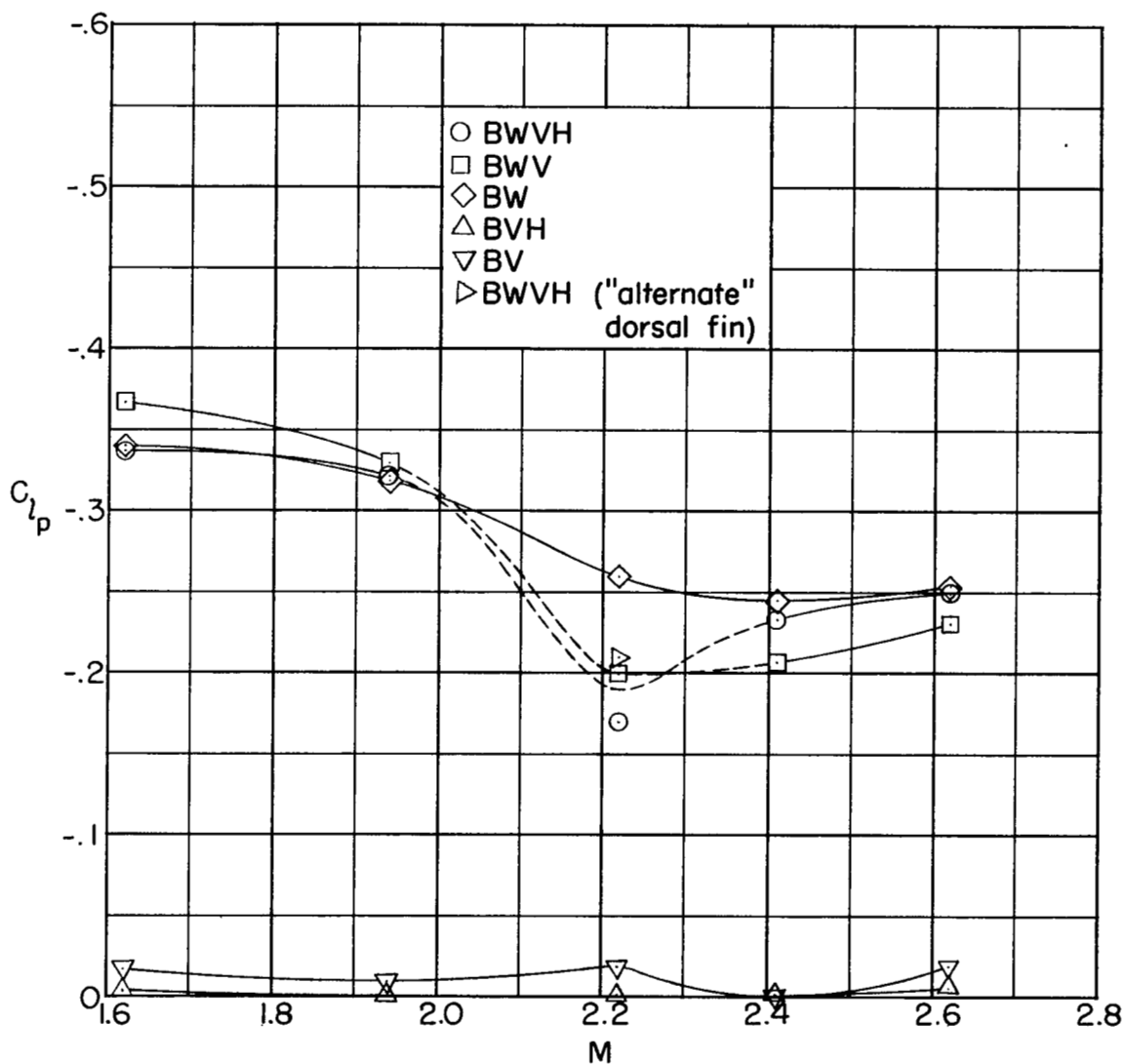


Figure 9.- Variations with Mach number of the damping in roll of the complete model and its components at zero angle of attack. Dorsal and ventral fins in place. Dashed portions of curves denote uncertain fairing.

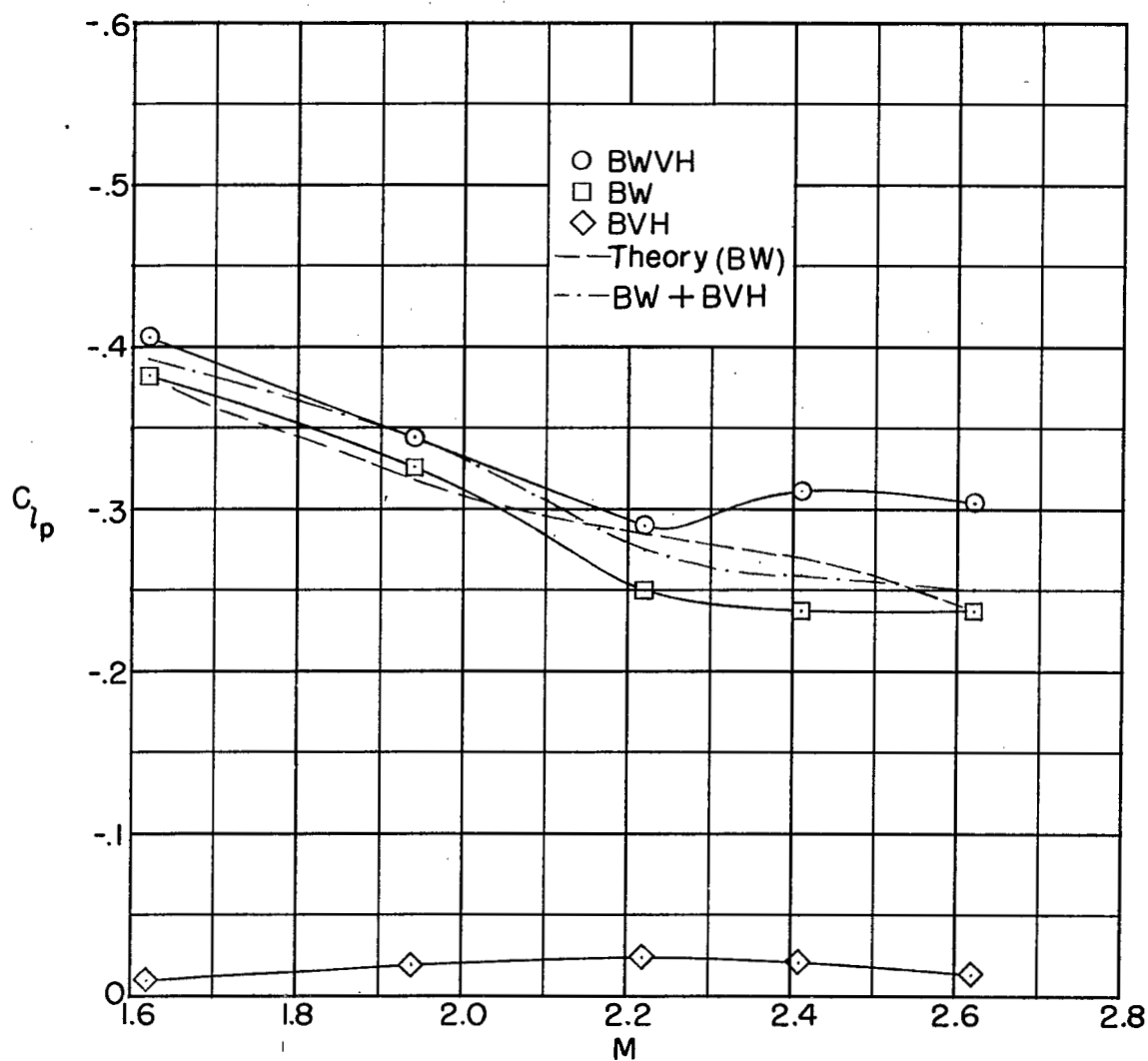


Figure 10.- Variations with Mach number of the damping in roll of the complete model and some of its components at zero angle of attack. Dorsal and ventral fins removed.

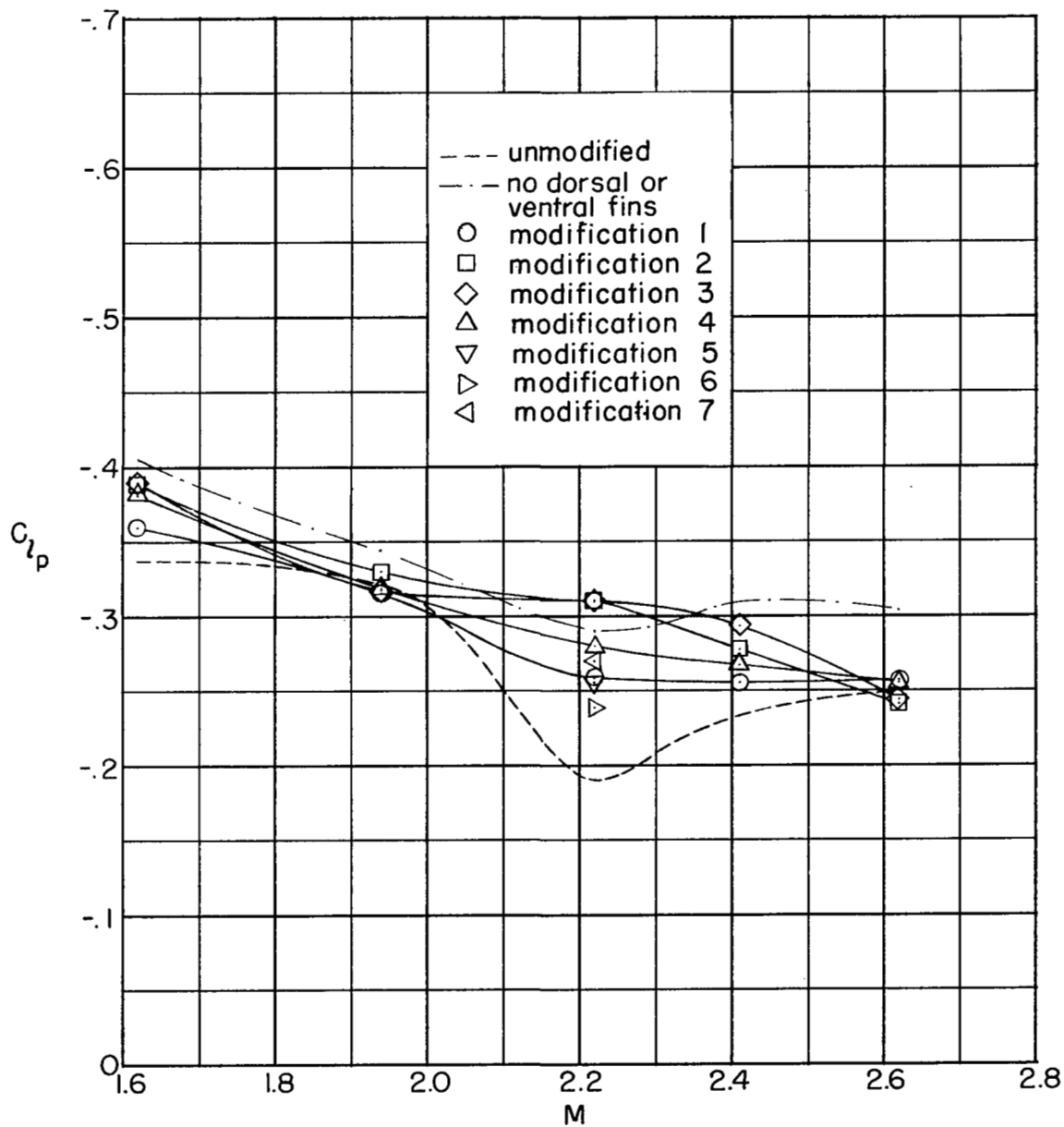


Figure 11.- Variations with Mach number of the damping in roll at zero angle of attack of the unmodified complete model and the complete model with various modifications to the dorsal and ventral fins.